Iron-Modified MCM-48 Mesoporous Molecular Sieves

Bousselham Echchahed,[†] Arild Moen,[†] David Nicholson,[‡] and Laurent Bonneviot*,[†]

Department of Chemistry
CERPIC, Laval University
Sainte Foy, G1K 7P4, Québec, Canada
Department of Chemistry
Norwegian University of Science and Technology
Rosenborg, N-7034 Trondheim, Norway

Received April 14, 1997
Revised Manuscript Received June 17, 1997

Five years ago, a novel family of mesoporous molecular sieves designated as M41S was discovered.[1,2] These materials, initially synthesized in their aluminosilicate and purely siliceous forms, are characterized by very large surface areas (1000−1400 m^2/g) and a very narrow pore size distribution. There are two well-defined porous phases in this family of materials. The first, MCM-41, has a hexagonal arrangement of monodimensional pores, while the second, MCM-48, displays a cubic structure indexed in the *Ia*3*d* space group recently modeled as a gyroid minimal surface.[3−6] Besides their well-ordered networks of channels, Raman and ^{29}Si NMR spectroscopies reveal that the pore wall should be considered as an amorphous array of corner sharing [MO_4] units (M = Si or Al).[7,8] Owing to their exceptional absorption capacities and molecular sieving properties, they are very attractive materials for the design of new heterogeneous catalysis. In that connection, acidic and redox functions can be introduced on incorporating heteroelements either as extraframework nanoscale oxide clusters or in their appropriate valence state as tetrahedral framework species. Both cases have been demonstrated for iron using UV−visible and X-ray absorption near-edge structure (XANES).[9,10] Framework iron has also been characterized in much less ordered siliceous HMS materials obtained using neutral surfactant templates (instead of ionic templates for the MS41 family).[11] Despite the very attractive structure of the MCM-48 with its 3D channel network, few studies of their modifications using heteroatoms have been reported and none, to our knowledge, concerns iron.[13−16] Furthermore, this phase exhibits a set of narrower XRD peaks which provides a more exigent criterion for channel ordering than the HMS or MCM-41 phases. A direct synthesis route for iron-modified MCM-48 is described here together with the results of a number of techniques used to probe both the host matrix framework and the iron environment.

The synthesis mixture was prepared using tetramethylammonium silicate 10% silica purchased from Sachem, tetraethyl orthosilicate (TEOS) 98%, cethyltrimethylammonium chloride (CTMA-Cl) 25 wt % aqueous solution and $Fe(NO_3)_3{\cdot}9H_2O$ from Aldrich. A solution of cetyltrimethylammonium hydroxide CTMA−Cl/OH was prepared by batch exchange of a 25 wt % aqueous solution of CTMA−Cl using the IRA-400(OH) ion-exchange resin (from Aldrich). A typical synthesis procedure was as follows: tetraethyl orthosilicate (5 g) and tetramethylammonium silicate (14.5 g; 10% silica) were added under stirring to cetyltrimethylammonium hydroxide (58 g). The stirring was continued for 60 min before the addition of the iron nitrate solution (prepared by dissolving 0.192 g of $Fe(NO_3)_3{\cdot}9H_2O$ in 4 g of water for Si/Fe = 100:1). The gel composition is $1SiO_2$, 0.48-$(CTMA)_2O$, 0.083 $(TMA)_2O$, $xFe_2O_3{\cdot}65H_2O$, with x = 0.005 and 0.0075.

The pure silica derivatives were synthesized according to the procedure of Beck et al.[3] This mixture was placed in a static autoclave for 48 h at about 100 °C. The solid was filtered off, washed with distilled water, dried at room temperature and, finally refluxed at 70 °C for 1 h in an ethanol solution of ammonium chloride. The resulting solid was then calcined in air with an heating rate of 1.5 °C/min up to a plateau of 6 h at 540 °C. Atomic absorption revealed that the Si/Fe ratios were 61 ± 4:1 and 40 ± 3:1 in the solid while they were 100:1 and 66.6:1 in the initial gel, respectively. The silicon deficit in the solid is attributed to an incomplete polycondensation of the silicon precursor leading to soluble species (ca. 33 mol % of Si) removed by filtration. After calcination, their respective BET surface areas of ca. 980 and 1000 m^2/g were measured from nitrogen adsorption−desorption isotherms performed using an Omnisorb 100. Comparatively, the BET surface area of our purely siliceous samples are ca. 1050 m^2/g. The pore size distribution obtained from the Barrer−Joyner−Halenda method is very similar for all the samples. They are characterized by a narrow single peak (fwhm of ca. 2.2 Å for iron-modified materials and ca. 2.7 Å for pure silica form) centered at 28 ± 1 Å typical of the M41S family.[3,5] All the XRD powder patterns exhibit two peaks at 2θ smaller than 3° and a series of weak peaks in range 3.5−5.5° as expected for a MCM-48 phase. They are assigned to the (211), (220), (400), (420), (332), and (431) reflections in the *Ia*3*d* space group (Figure 1).[3,4−6] After calcination (Figure 1b,d) the

* To whom correspondence should be addressed.
[†] Laval University.
[‡] Norwegian University of Science and Technology.

(1) Kresge, C. T.; Leonwicz, M. E.; Roth, W. J.; Vartuli, J. C.; Beck, J. S. *Nature* **1992**, *359*, 710.
(2) Beck, J. S.; Vartuli, J. C.; Roth, W. J.; Leonwicz, M. E.; Kresge, C. T.; Schmitt, K. D.; Chu, C. T.-W.; Olson, D. H.; Sheppard, E. W.; McCullen, S. B.; Higgins, J. B.; Schlenker, J. L. *J. Am. Chem. Soc.* **1992**, *114*, 10834.
(3) Vartuli, J. C.; Schmitt, K. D.; Kresge, C. T.; Roth W. J.; Leonwicz, M. E.; McCullen, S. B.; Hellring, S. D.; Beck, J. S.; Schlenker, J. L.; Olson, D. H.; Sheppard, E. W. *Chem. Mater.* **1994**, *6*, 2317.
(4) Monnier, A.; Schüth, F.; Kumar, Q.; Margolese, D.; Maxwell, R. S.; Stucky, G. D.; Krishnamurty, M.; Petroff, P.; Firouzi, A.; Janicke, M.; Chemelka, B. F. *Science* **1993**, *261*, 1299.
(5) Schmidt, R.; Hansen, E. W.; Stöcker, M.; Akporiaye, D.; Ellestad, O. H. *Microporous Mater.* **1995**, *3*, 443.
(6) Alfredsson, V.; Anderson, M. W. *Chem. Mater.* **1996**, *8*, 1141.
(7) Chen, C.-Y.; Li, H.-X.; Davis, M. E. *Microporous Mater.* **1993**, *2*, 17.
(8) Luan, Z.; Cheng, C.-F.; Zhou, W.; Klinowski, J. *J. Phys. Chem.* **1995**, *99*, 1018.
(9) Abe, T.; Tachibana, Y.; Uematsu, T.; Iwamoto, M. *J. Chem. Soc., Chem. Commun.* **1995**, 1617.
(10) Rey, F.; Sankar, G.; Maschmeyer, T.; Thomas, J. M.; Bell, R. B.; Greaves, G. N. *Top. Catal.* **1996**, *3*, 121.
(11) Tuel, A.; Gontier, S. *Chem. Mater.* **1996**, *8*, 114.
(12) Huo, Q.; Margolese, D. I.; Stucky, G. D. *Chem. Mater.* **1996**, *8*, 1147.
(13) Schmidt, R.; Junggreen, H.; Stöcker, M. *J. Chem. Soc., Chem. Commun.* **1996**, 875.
(14) Zhang, W.; Pinnavaia, T. J. *Catal. Lett.* **1996**, *38*, 261.
(15) Morey, M.; Davidson, A.; Stucky, G. D. *Microporous Mater.* **1996**, *6*, 99.
(16) Zhao, D.; Goldfarb, D. *J. Chem. Soc., Chem. Commun.* **1995**, 875.

S0897-4756(97)00241-X CCC: $14.00

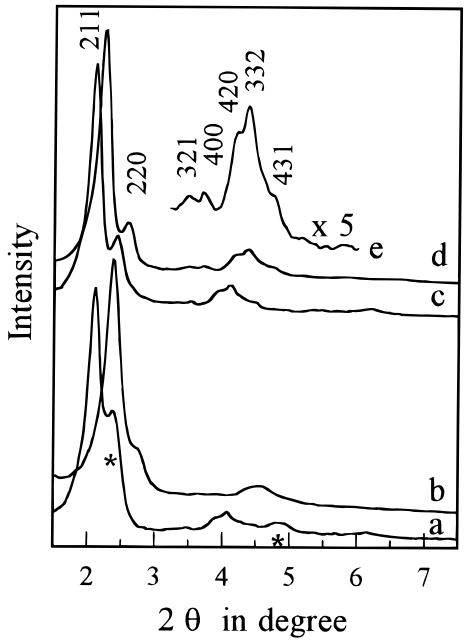

Figure 1. X-ray diffraction patterns of Fe−MCM-48 with Si/Fe = 61:1 (a) as-synthesized (* traces of lamellar MCM-50 phase disappearing after calcination), (b) calcined and (c) and (d) as (a) and (b) for Si/Fe = 40:1.

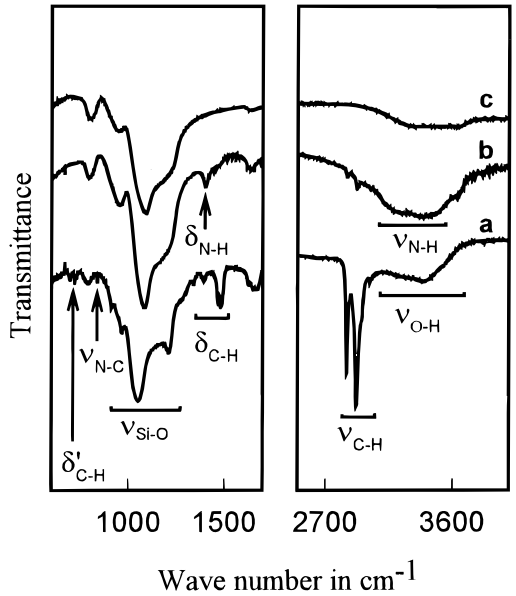

Figure 2. FT-IR spectra of (a) as-synthesized, (b) treated with NH_4Cl solution, and (c) calcined Fe−MCM-48 with Si/Fe = 61:1; ν, δ, and δ' stand for stretching, bending, and wagging modes, respectively, for $CTMA^+$ (C−H, CH_2, and N−C), for NH_4^+ (N−H) and for SiO_4 units (Si−O).

d_{hkl} spacing decreases from 42 to 38 ± 2 Å. The accuracy of the XRD measurement was not sufficient to differentiate the iron-modified and the pure silica form material. The IR spectra reveal that the $CTMA^+$ ions have been almost completely removed (ca. 95%) after reflux in the ethanol NH_4Cl solution (Figure 2). Similar observations were reported for MCM-41 and HMS materials using either HCl or NaCl.[7,11] In addition, here, the presence of characteristic N−H bands in the treated materials suggest that $CTMA^+$ has been ion exchanged by NH_4^+ while the absence of iron in the filtrate indicates that there was no exchangeable iron species.

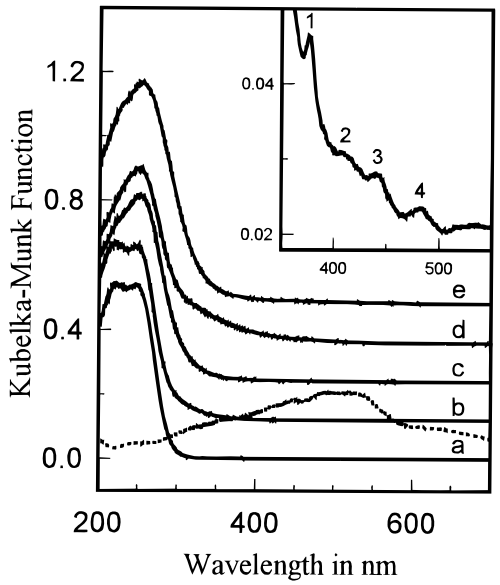

Figure 3. Diffuse reflectance UV−vis spectra of Fe−MCM-48 diluted (20%) in MgO using pure MgO as a reference: (a) as-synthesized for Si/Fe = 61:1, (b) ion exchanged, (c) ion exchanged and calcined, (d) calcined without template removal, and (e) ion exchanged and calcined for Si/Fe = 40:1; insert as (a) with a dilution in MgO of 50%; (dotted line) Fe_2O_3 diluted in MCM (equivalent loading 3 mol %).

The UV−visible reflectance spectra were recorded on a Perkin-Elmer Lambda 5 spectrometer equipped with a Harricks reflectance attachment and reported using the Kubelka−Munk function $[F(R_\infty)]$ (Figure 3). The white as-synthesized materials are characterized by a very intense band in the UV range comprising two components at ca. 240 and 260 nm that are shifted toward higher wavelengths by ca. 10 nm and less resolved in the calcined form. There are four very weak and narrow bands in the visible region arising at 375, 415, 442, and 482 nm, each with a fwhm of ca. 15 nm (Figure 2, insert). The former group of bands are assigned to Laporte allowed ligand to metal electron-transfer transitions and the latter to spin forbidden d−d transitions (crystal field splitting of ca. 8500 cm^{-1}) consistent with tetrahedral sites in agreement with previous studies on $FePO_4$, Fe−HMS, and FeS-1 silicalites.[17−19] The absence of broad bands in the visible region reveals that there is neither iron(II) nor ferric oxide Fe_2O_3 species in the as-synthesized samples.[19] However, the materials calcined with the $CTMA^+$ ions turn yellowish due to an absorption at about 350 nm. This might be due to nanoscale iron oxide clusters whose absorption is expected to be blue-shifted according to the quantum size effect.[9,20] In the following, the data are reported only for the Si:Fe ratio of 61:1, since there is no significant difference for both iron contents.

The electron spin resonance spectra of Fe−MCM-48 are very similar to those of FeS-1[17,19] and Fe−HMS[11] in which most of the iron species are isolated paramag-

(17) Lin, D. H.; Coudurier, G.: Vedrine, J. C. *Stud. Surf. Sci. Catal.* **1989**, *49*, 1431.
(18) Patarin, J.; Tuilier, M. H.; Durr, J.; Kessler, H. *Zeolites* **1992**, *12*, 70.
(19) Bordiga, S.; Buzzoni, R.; Geobaldo, F.; Lamberti, C.; Giamello, E.; Zecchina, A.; Leofani, G.; Petrini, G.; Tozzola, G.; Vlaic, G. *J. Catal.* **1996**, *148*, 486.
(20) Trong On, D.; Kaliaguine, S.; Bonneviot, L. *J. Catal.* **1995**, *157*, 235.

Table 1. Preedge Peak Characteristics of 1% Fe−MCM-48 and References

		preedge peak[b]			
sample	state[a]	position[d] ± 0.1 eV	line width ± 0.05 eV	intensity[e] ± 5%	tetrahedral[c] sites ± 10%
Fe_2O_3[f]	polycryst	7113.8	2.86	48	0
		7115.8	1.40	10	
		7117.1	1.40	13	
$FePO_4$	polycryst	7113.6	1.85	100	100
MCM-48	as-synth	7113.5	1.93	87	83
	exch + calc + hydr	7113.5	1.87	76	60
	exch + calc + deshydr	7113.3	1.82	78	65
	direct calc	7113.5	2.25	56	35

[a] polycryst = polycrystalline, as-synth = as synthesized, exch = NH_4^+ ion exchanged, calc = calcined, deshydr = (des-)hydrated. [b] Obtained from Gaussian fit with baseline correction of preedge peak ($R_{fit} > 0.997$). [c] From best edge fit using calculated edge of a $(FePO_4)_x$·$(Fe_2O_3)_{1-x}$ mixture; see Figure 4 for corresponding match on the overall edge. [d] Energy calibration at the first inflection point of metal foil edge taken at 7112 eV. [e] Surface normalized to 100 for $FePO_4$ whose prepeak height was of ca. 0.14 after baseline correction and surface area of ca. 0.28 ± 0.02 (in agreement with ref 19). [f] Asymmetrical preedge, three Gaussian fit (average position and line width 7114.5 and 4.9 eV, respectively).

netic sites. Conversely, when the materials are not ion exchanged by NH_4^+ ions prior to calcination, there is a broad antiferromagnetic signal consistent with nanoscale oxide clusters mentioned above. According to their sizes, they are likely confined within the channel of the structure. However, the ESR signal does not yield the coordination number which is a key parameter.[21]

XANES measurements were therefore performed at the Fe K-edge using the synchrotron facilities at Daresbury (SRS, station 7.1) and at LURE (DCI, station D42). A double-crystal silicon(111) monochromator detuned (50%) for harmonic rejection was used to scan the X-ray photon stepwise by 0.2 eV. Ion chambers filled with a partial pressure of argon were used to detect the intensities of the incident and transmitted X-ray beams. The normalization of the edges to the height of the absorption step allows us to compare the peak intensities for different phases and eventually to quantify phase mixtures.[20] The preedge intensity, the XANES profile and the edge position deeply depends on the symmetry, on the bond length and on the oxidation state of the absorber atom.[22] The half-height edge step position is characteristic of iron(III) for all the samples [iron(II) edge positions arise at ca. 2 eV lower]. For comparison, Fe_2O_3 and $FePO_4$ nonporous and crystalline phases were taken as references for octahedral and tedrahedral iron(III) sites, respectively. At low energies, a single preedge peak arises at 7113.5 eV for $FePO_4$ and for Fe−MCM-48 (Figure 4, insert). However, the peak intensity is smaller particularly for materials calcined with their channels full of $CTMA^+$ ions. The postedge may eventually resemble more that of Fe_2O_3 than that of $FePO_4$. Though one may argue that a slightly weaker preedge for iron sites in MCM may be due to distortion,[10] intermediate characteristics are more likely due to the presence of a mixture of coordination states. The edge of the Fe−MCM-48 can indeed be simulated using a linear combination of the edges of both references. The fits provide semiquantitative site distribution showing that the MCM-48 predominantly contains tetrahedral sites except when calcination has been carried out without removal of the template (Table 1). The slight imperfections of the fit is attributed to the approximations made in using reference compounds to simulate real iron sites. In addition, very small increases of the preedge after dehydration indicate that less than 5% of the sites are involved in a change of coordination number as it is the case in iron silicalites.[19]

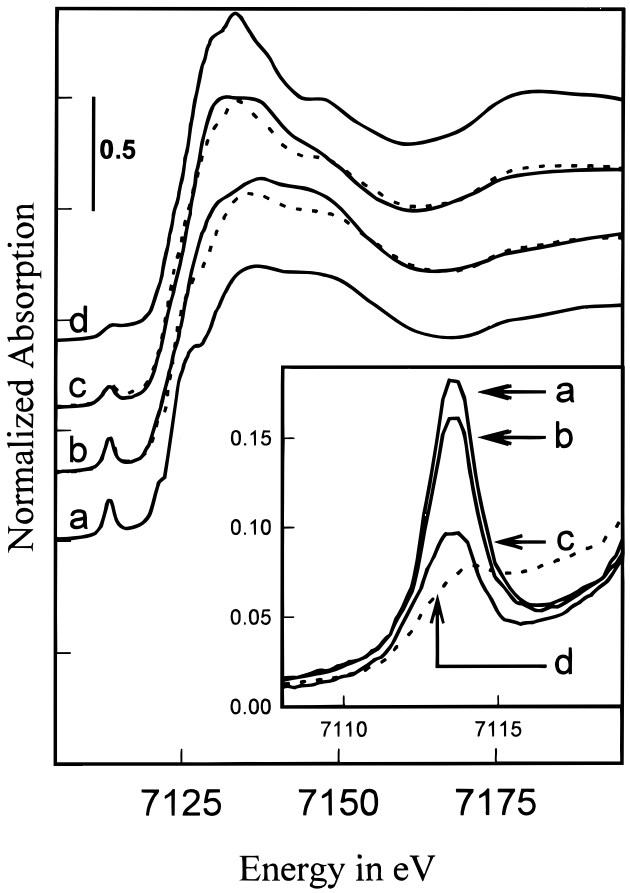

Figure 4. XANES spectra of (a) $FePO_4$, (b) as-synthesized Fe−MCM-48 with Si/Fe = 61:1, (c) same as (b) after calcination without ion-exchange removal of $CTMA^+$ and (d) Fe_2O_3; dash lines represent the edges obtained by linear combination of the edges of the references (see Table 1); insert: details of the preedge region.

Iron-modified siliceous MCM-48 phases have been synthesized where iron(III) ions mostly occupy tetrahedral sites within their siliceous walls. The formation of oxide nanoclusters in the channels is favored in the presence of the organic template molecules during calcination. The role of the template on iron aggregation and the effect of the iron content will be reported in a forthcoming paper.

(21) Goldfarb, D.; Bernardo, M.; Strohmaier, K. G.; Vaughan, D. E. W.; Thomann, H. *J. Am. Chem. Soc.* **1994**, *116*, 6344.

(22) Henderson, C. M. B.; Gressey, G.; Redfern, S. A. T. *Radiat. Phys. Chem.* **1995**, *45*, 459.

Acknowledgment. This work was supported by NSERC and FCAR in Canada. Daresbury Laboratory in UK and LURE in France are also thanked for providing beam time. Support from the Norwegian Research Council (including a NATO Postdoctoral Fellowship to A.M.), the Nansen Foundation, and VISTA-Statoil (to D.G.N.) is much appreciated.

CM970241E